+ MODEL

Genes & Diseases (2024) 11, 101148

Available online at www.sciencedirect.com

ScienceDirect

journal homepage: www.keaipublishing.com/en/journals/genes-diseases

FULL LENGTH ARTICLE

XBP1 splicing contributes to endoplasmic reticulum stress-induced human islet amyloid polypeptide up-regulation

Yun Zhang [a,**,1], Susan Lin [b,1], Jing Yao [a,1], Wantong Cai [c,d], Huaqiu Chen [a], Ailikemu Aierken [a], Zhe Wang [a], Weihong Song [a,b,c,d,*]

[a] National Clinical Research Center for Geriatric Disorders, Xuanwu Hospital, Capital Medical University, Beijing 100053, China
[b] Townsend Family Laboratories, Department of Psychiatry, The University of British Columbia, 2255 Wesbrook Mall, Vancouver, BC V6T 1Z3, Canada
[c] Institute of Aging, Key Laboratory of Alzheimer's Disease of Zhejiang Province, School of Mental Health and the Affiliated Kangning Hospital, Wenzhou Medical University, Wenzhou, Zhejiang 325000, China
[d] Oujiang Laboratory (Zhejiang Lab for Regenerative Medicine, Vision and Brain Health), Wenzhou, Zhejiang 325001, China

Received 30 May 2022; received in revised form 20 June 2023; accepted 16 September 2023
Available online 19 October 2023

KEYWORDS
β-cell function;
Endoplasmic reticulum stress;
Islet amyloid polypeptide;
Type 2 diabetes mellitus;
XBP1

Abstract As a pathological hallmark of type 2 diabetes mellitus (T2DM), islet amyloid is formed by the aggregation of islet amyloid polypeptide (IAPP). Endoplasmic reticulum (ER) stress interacts with IAPP aggregates and has been implicated in the pathogenesis of T2DM. To examine the role of ER stress in T2DM, we cloned the hIAPP promoter and analyzed its promoter activity in human β-cells. We found that ER stress significantly enhanced hIAPP promoter activity and expression in human β-cells via triggering X-box binding protein 1 (XBP1) splicing. We identified a binding site of XBP1 in the hIAPP promoter. Disruption of this binding site by substitution or deletion mutagenesis significantly diminished the effects of ER stress on hIAPP promoter activity. Blockade of XBP splicing by MKC3946 treatment inhibited ER stress-induced hIAPP up-regulation and improved human β-cell survival and function. Our study uncovers a

* Corresponding author. National Clinical Research Center for Geriatric Disorders, Xuanwu Hospital, Capital Medical University, Beijing 100053, China.
** Corresponding author.
E-mail addresses: zhangyun@xwhosp.org (Y. Zhang), weihong@wmu.edu.cn (W. Song).
Peer review under responsibility of Chongqing Medical University.
[1] These authors contributed equally to this work.

https://doi.org/10.1016/j.gendis.2023.101148

link between ER stress and IAPP at the transcriptional level and may provide novel insights into the role of ER stress in IAPP cytotoxicity and the pathogenesis of T2DM.

Introduction

Endoplasmic reticulum (ER) stress and the downstream unfolded protein response (UPR) activation have been linked to obesity and type 2 diabetes mellitus (T2DM) development in mouse models,[1] carving out a prominent role for ER stress in T2DM pathogenesis.[2] X-box binding protein 1 (XBP1) was identified to be a stress-inducible transcription factor that is ubiquitously expressed in adult tissues.[3] Under physiological conditions, expression of unspliced XBP1 (XBP1u) in the cytoplasm is kept quite low, given the instability and short half-life of the protein. Under periods of ER stress, XBP1 transcription is enhanced, resulting in increased XBP1 splicing by IRE1.[4] In pancreatic islet β-cells, an increase in XBP1 splicing leads to cell apoptosis and decreased insulin secretion.[5]

Islet amyloid is a pathological hallmark of T2DM and occurs in over 95% of T2DM patients.[6] It is formed by the aggregation of islet amyloid polypeptide (IAPP), which is synthesized by the sequential cleavages of an 89-amino acid preproIAPP (Fig. 1A). The mechanism underlying IAPP aggregation is largely unknown; however, animal studies have shown that overexpression of human IAPP (hIAPP) leads to amyloid deposition,[7] suggesting that the amount of hIAPP produced and secreted by β-cells may play a role in its amyloidogenesis.[8] This idea is bolstered by the observation that suppression of endogenous hIAPP synthesis using small interfering RNA (siRNA) can inhibit amyloid formation and its cytotoxicity.[9] Previous studies examining *hIAPP* gene transcription have revealed complex promoter regulation mechanisms. However, a pervading question remains of how, or if, *hIAPP* transcription can be altered in pathogenic states, especially within T2DM contexts.

In this brief report, we demonstrated that ER stress significantly enhanced *hIAPP* promoter activity by inducing XBP1 splicing. Disruption of the binding site or reduction of spliced XBP1 significantly decreased *hIAPP* promoter activity and its expression, which improved human pancreatic β-cell survival and function.

Materials and methods

Cloning and plasmids

Cloning primers for the human IAPP gene promoter were designed with restriction sites for insertion into the multiple cloning sites of the pGL3-basic vector (Promega). Promoter fragments from −1618 base pairs (bp) upstream to +450 bp downstream of the transcription start site were PCR-amplified from HEK293 genomic DNA with the following primers: forward: MluI-1618, 5′-aatttggtctggtgttcaagcc; MluI-553, 5′-tacctagaataatccctaccacag; MluI-240, 5′-ggcaaattcaaacttctgctgtg; MluI-163, 5′-actgatgagttaatgtaataatgaccc; MluI-65, 5′-tgcctgatgtcagagctgag; reverse: XhoI+435, 5′-ctgcaaagaataatccagcac; XhoI+450, 5′-tgcttctcaaattttctgcaaaga. pIAPP-luc −1007/+435 was cloned by restriction enzyme digest of the pIAPP-luc −1618/+435 plasmid at a unique SmaI site. Mutant constructs were generated with overlap extension PCR using the following primers: 175Mut-Forward, 5′-cactgtgtatttgctgtcttaatatttactg; 175Mut-Reverse, 5′- cagtaaatattaagacagcaaatacacagtg; 175Del-Forward: 5′- cactgtgtatttgcttaatatttactgatg; 175Del-Reverse: 5′- catcagtaaatattaagcaaatacacagtg. Cloning primers for expression plasmids were designed with restriction sites for insertion into the multiple cloning site of the pcDNA4-mycHisA vector (Promega). The following primers were used: XBP1u-myc, HindIII-5′-atggtggtggtggcagcc and XhoI-5′- gttcattaatggcttccagcttggct; XBP1s-myc, HindIII-5′- atggtggtggtggcagcc and XhoI-5′-gacactaatcagctggggaaaga.

Cell culture and drug treatment

1.1B4 cells were purchased from Sigma—Aldrich and cultured in Roswell Park Memorial Institute (RPMI 1640) medium supplemented with 10% FBS, 2 mM L-glutamine, 100 units penicillin, and 100 μg streptomycin (Invitrogen). Tunicamycin (Sigma) was dissolved in dimethyl sulfoxide (DMSO) at a stock concentration of 10 mg/mL and added at a dilution of 1:1000 (10 μg/mL) to the cell culture medium for 24 h to induce ER stress. Thapsigargin (MCE) was also dissolved in DMSO at a stock concentration of 1 mM and added at a dilution of 1:1000 (1 μM) to the cell culture medium to induce ER stress. MKC3946 (TargetMol) was dissolved in DMSO at a stock concentration of 10 mM and was added at a dilution of 1:1000 (10 μM) to the cell medium to inhibit XBP1 splicing.

Dual-luciferase reporter assay

Cells were seeded onto 24 well plates and co-transfected with 500 ng luciferase plasmid and 1 ng Renilla luciferase plasmid (pRL-CMV) to normalize for transfection efficiency. For triple co-transfections, 250 ng of each plasmid and 1 ng pRL-CMV were transfected. Firefly and Renilla luciferase activities were sequentially assayed using the dual-luciferase reporter system (Promega) with a luminometer (Turner BioSystems TD-20/20). Firefly luciferase activity was normalized to Renilla luciferase activity and expressed as relative luciferase units (RLU).

RT-PCR

Total RNA was extracted from 1.1B4 cells with TRI reagent (Sigma). 1.0 μg of total RNA was synthesized into first strand cDNA with the Thermoscript™ RT-PCR system (Invitrogen). The newly synthesized cDNA was further amplified by Taq DNA polymerase and products were resolved on 1%—2% agarose gels. The following primers were used for RT-PCR: IAPP, 5′-cccattgaaagtcatcaggtgg and 5′-tggatcccacgttggtagat; XBP1, 5′- ccttgtagttgagaaccagg and 5′-ggtccaagttgtccagaatgc; GAPDH, 5′- ggatttggtcgtattggg and 5′- ggaagatggtgatgggatt; Beta-actin, 5′- ggacttcgagcaagagatgg and 5′-gaagcatttgcg-gtggag.

Immunoblot analysis

Cells were lysed in RIPA-DOC lysis buffer supplemented with a complete Mini Protease Inhibitor Cocktail Tablet (Roche Diagnostics). The samples were diluted in 4 × SDS-sample buffer, boiled, and resolved on 8% or 10% tris-glycine SDS-PAGE gels and transferred to Immobilon-FL PVDF membranes. The membranes were blocked with 5% BSA, followed by overnight incubation with primary antibodies at 4 °C. Rabbit anti-IRE1 (Proteintech) and anti-phospho-IRE1α (Beyotime) polyclonal antibodies were used to detect total IRE1 and phosphorylated IRE1 levels, respectively. CHOP was detected by mouse anti-CHOP monoclonal antibody (Cell Signaling). ATF4 was determined using rabbit anti-ATF4 polyclonal antibody (Proteintech). The ratio of cleaved (active) caspase 3/total caspase 3 was evaluated using cleaved caspase 3 (Asp175) antibody and caspase 3 (D3R6Y) rabbit monoclonal antibody, respectively (Cell Signaling). Internal control β-actin was analyzed using the monoclonal antibody AC-15 (Sigma—Aldrich). Internal control GADPH was analyzed using monoclonal antibody 14C10 (Cell Signaling). The blots were scanned using the Odyssey Imager (LI-COR Bioscience).

Immunolabelling

Cells were incubated at 4 °C overnight with rabbit anti-IAPP (1:200). They were then washed with PBS, incubated for 1 h at room temperature with Texas red-conjugated anti-rabbit (1:500), and counterstained with the nuclear dye DAPI (Vector Laboratories). For TUNEL staining, cells were incubated at 37 °C for 60 min with a TUNEL reaction mixture (1:20; Roche Diagnostics).

Human IAPP (amylin) ELISA

Cell culture media were collected and prepared according to the manufacturer's instructions. The concentration of human IAPP (amylin) was detected using the competitive enzyme immunoassay technique (CEA812Hu-Cloud-Clone Corp).

Glucose-stimulated insulin secretion

Cells were pre-incubated at 37 °C for 1 h in KRB buffer containing 10 mmol/L HEPES (pH 7.4), 0.25% BSA (w/v), and 1.67 mmol/L glucose, followed by 1-h incubation in KRB containing 1.67 mmol/L glucose (basal insulin release) and another hour in KRB containing 16.7 mmol/L glucose (stimulated insulin release). Cells were lysed in a buffer containing 1 mol/L acetic acid/0.1% BSA (10 min, 100 °C). Insulin levels were measured by a human-specific insulin ELISA kit (Cloud-Clone Corp).

Statistical analysis

All statistical analyses were performed using GraphPad Prism 7 software. All results and error bars are presented as mean ± standard error of the mean. For two-group comparisons, results were analyzed by a two-tailed student's *t*-test. For multiple-group comparisons, results were analyzed by one-way analysis of variance (ANOVA) or two-way ANOVA. Statistical significance was accepted when $P < 0.05$.

Results

ER stress stimulated hIAPP biosynthesis and human β-cell apoptosis

To examine the effect of ER stress on hIAPP biosynthesis and secretion, tunicamycin or thapsigargin was applied to human β-cell line 1.1 B4. Compared with cells treated with DMSO as controls, cells treated with tunicamycin or thapsigargin had a profound increase in p-IRE1/t-IRE1 levels (4.4 folds and 6.9 folds, respectively) and CHOP levels (44.2 folds and 28.1 folds, respectively) (Fig. 1B), indicating the successful activation of ER stress. As a stress-induced transcription factor, activating transcription factor 4 (ATF4) levels were also significantly elevated in the cells treated with tunicamycin or thapsigargin (2.7 folds and 2.8 folds, respectively) (Fig. 1B). More importantly, ER stress induced by tunicamycin or thapsigargin treatment markedly increased the levels of human IAPP to 134% ± 7.39% ($P = 0.0102$) and 127% ± 5.2% ($P = 0.0069$), respectively (Fig. 1C, D). These results demonstrated that tunicamycin-induced ER stress increased hIAPP biosynthesis. To further investigate whether these pathological processes affect human β-cell viability and function, we examined caspase 3 activation and DNA fragmentation. Compared with the controls, the ratio of cleaved (active form) caspase 3/total caspase 3 in tunicamycin-treated or thapsigargin-treated cells significantly increased with 5.4 folds and 2.2 folds, respectively (Fig. 1B). The number of TUNEL-positive cells was also markedly increased to 380.6% ± 61.89% ($P < 0.05$) (Fig. 1E) in tunicamycin-treated cells.

ER stress up-regulated *hIAPP* promoter activity

To examine whether ER stress-regulated *IAPP* vis its effect on transcriptional activation, a 2053 bp of the *hIAPP* gene's 5′ flanking region spanning −1618 bp upstream of the transcription start site and +435 bp downstream of the transcription start site was cloned into pGL3-basic (Fig. 2A). Plasmid vector pGL3-basic contains a luciferase reporter and lacks a eukaryotic promoter; expression of the firefly

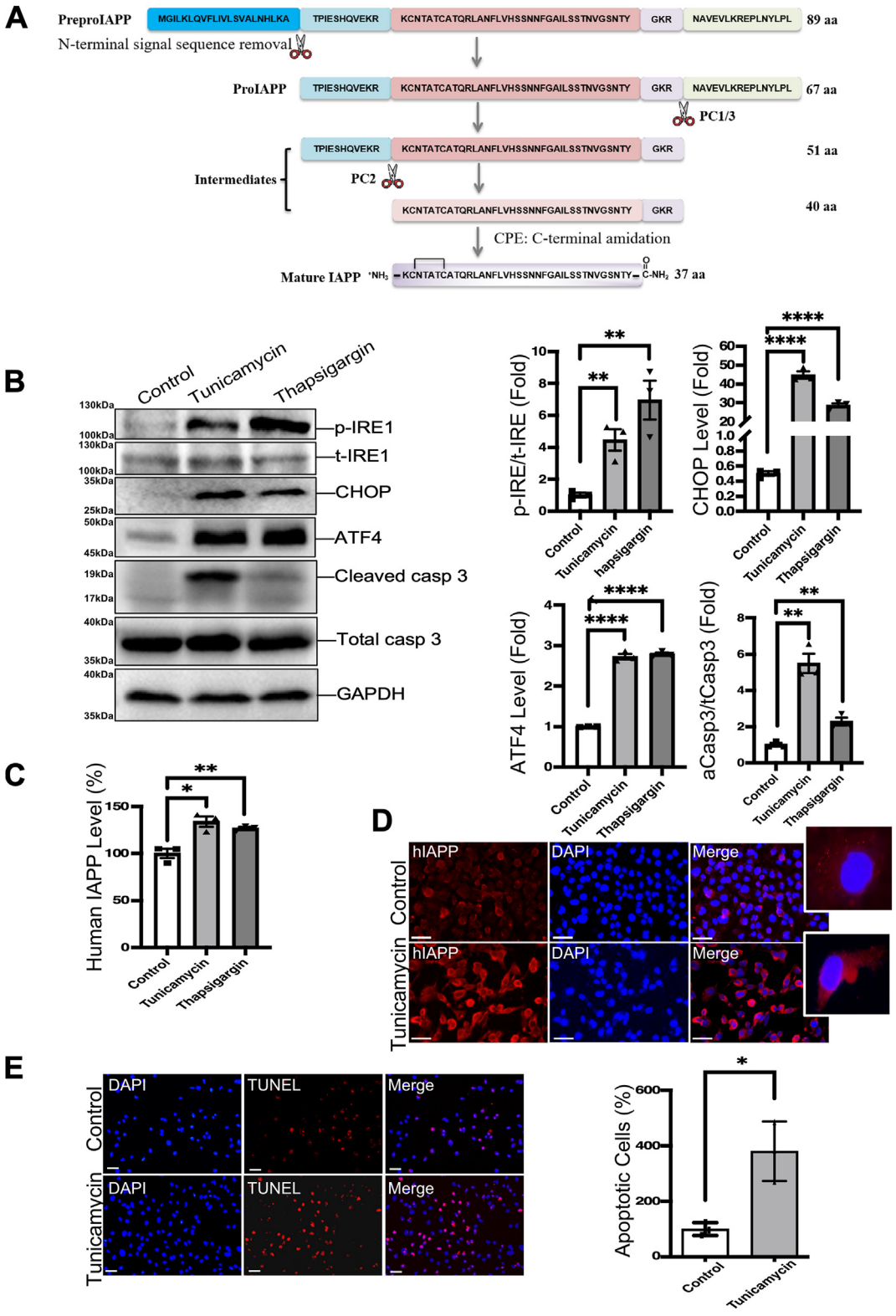

Figure 1 The effect of tunicamycin and thapsigargin on hIAPP biosynthesis and human β-cell viability. **(A)** The schematic diagram showing the processing of preproIAPP to mature IAPP. IAPP is first synthesized in the ER as an 89-amino acid preproIAPP. A 67-amino acid proIAPP is subsequently formed after the removal of a 22-amino acid N-terminal signal peptide. ProIAPP (8 kDa) is further cleaved in the Golgi by prohormone convertase 1/3 (PC1/3) followed by PC2-mediated cleavage of the N-terminus in the secretory granules. Finally, the 37-amino acid mature IAPP is formed after C-terminal amidation by carboxypeptidase E (CPE) **(B)** 1.1B4 human β-cells were treated with 10 μg/mL tunicamycin, 1 μM thapsigargin or DMSO (controls) for 24 h. Cell lysates were resolved in SDS-PAGE gels. p-IRE1 and t-IRE1were detected by rabbit anti-IRE1 (phosphor S724) and rabbit anti-IRE1 antibodies, respectively.

luciferase protein is driven by any functional promoter correctly inserted upstream of the gene.

Deletion constructs covering varying lengths of the 5′ flanking region of the *hIAPP* gene were generated (Fig. 2B). The −1618/+450, −1618/+435, and −1007/+435 constructs had significantly low luciferase activity in human β-cells (Fig. 2C). However, the −553 to +435 fragment had approximately ten-fold higher luciferase activity compared with the empty vector (11.15 ± 1.354 RLU, $P < 0.0001$). In addition, removing 313 bp from the 5′ end of the −553/+435 construct generated a −240/+435 fragment, and this construct had significant luciferase activity compared with pGL3-basic (16.57 ± 3.059 RLU, $P < 0.0001$) and with the −553/+435 construct ($P = 0.0461$). Further deletion to create a −163/+435 construct abolished luciferase activity, with a mean RLU of 4.994 ± 0.3463 ($P = 0.1492$), namely, a four-fold drop in activity with deletion of only 77 nucleotides from the 5′ flanking region. A short −65/+435 construct also had no significant luciferase activity compared with pGL3-basic (2.427 ± 0.5158 RLU, $P = 0.9322$). As expected, a +435/−240 spanning fragment which was cloned into the pGL3-basic vector in reverse orientation had no promoter activity (0.05319 ± 0.005577 RLU, $P = 0.9786$).

To determine whether ER stress regulates *hIAPP* promoter activity, human β-cell 1.1B4 cells were transfected with *hIAPP* promoter construct −553/+435 and treated with tunicamycin. Tunicamycin treatment significantly increased *hIAPP* promoter activity (9.113 ± 1.115 RLU) compared with DMSO treatment (6.168 ± 0.2617 RLU, $P = 0.0331$) (Fig. 2D). To further identify the effect of ER stress on *hIAPP* transcription, RT-PCR was then performed to examine the mRNA levels. The level of *hIAPP* mRNA expression was significantly increased in tunicamycin-treated cells compared with DMSO controls (1.364 ± 0.09 fold change, $P = 0.0161$) (Fig. 2E).

ER stress-induced XBP1 splicing enhanced *hIAPP* transcription

ER stress activates the UPR, which consists of three parallel signaling pathways mediated by IRE1, PERK, and ATF6. The most conserved branch of UPR is IRE1 activation leading to the unconventional splicing of *XBP1* mRNA to generate spliced XBP1 (XBP1s). Although β-cells normally have a basal level of XBP1 splicing due to its high secretory demands, there was no evidence of XPB1 splicing in the DMSO-treated cells. However, tunicamycin treatment for 24 h successfully induced *XBP1* mRNA splicing with increased *XBP1s* mRNA expression (Fig. 3A).

Since ER stress can enhance the luciferase activity of the *hIAPP* −553/+435 promoter construct, we employed a computational transcription factor search (PROMO) for this 5′ flanking region. The PROMO results revealed a plethora of putative binding sites for different transcription factors such as Sp1, NFκB, and HIF-1. There are putative XBP1s binding sites at position −226 to −221 bp (ATGACAC) and at position −177 to −171 bp (GCTACGT) (Fig. 3B); thus, the unspliced and spliced isoforms of XBP1 (XBP1u and XBP1s, respectively) were co-transfected with hIAPP promoter constructs in 1.1B4 cells to elucidate their effects on hIAPP transcription. The shortest promoter construct, −65/+435, did not have a significant response to either XBP1u or XPB1s overexpression compared with the empty vector control (XBP1u: 1.071 ± 0.034 fold change, $P = 0.9994$; XBP1s: 3.123 ± 0.214 fold change, $P = 0.3695$) (Fig. 3C). Similarly, the −163/+435 construct co-transfected with either XBP1u or XBP1s did not have significant differences in promoter activity from the empty vector control (XBP1u: 1.07 ± 0.042 fold change, $P = 0.9997$; XBP1s: 4.076 ± 0.09 fold change, $P = 0.5616$). However, the −240/+435 promoter fragment displayed significantly increased luciferase activity when co-transfected with XBP1s (60.303 ± 12.526 fold change, $P < 0.0001$) but not with XBP1u (5.093 ± 0.382 fold change, $P = 0.8030$). The longer −1618/+435 construct also had a significant increase in promoter activity when co-transfected with XBP1s (31.778 ± 7.825 fold change, $P = 0.0003$) but not with XBP1u (2.344 ± 0.524 fold change, $P = 0.9573$) (Fig. 3C). XBP1u-myc, XBP1s-myc, or an empty vector was then transfected separately into 1.1B4 cells for RT-PCR (Fig. 3D). XBP1s overexpression significantly increased *hIAPP* mRNA compared with the empty vector control after normalization to internal controls (2.151 ± 0.1697 fold change, $P = 0.0036$), but XBP1u overexpression did not (1.623 ± 0.2249 fold change, $P = 0.0753$) (Fig. 3E). Taken together, these results suggest that XBP1s rather than XBP1u significantly increases *hIAPP* promoter activity and transcription.

To further confirm the effect of XBP1 on *hIAPP* promoter activation, mutation and deletion constructs of the *hIAPP* −240/+435 promoter fragment were generated (Fig. 3F). Mutating three nucleotides (ACG to GTC) of the binding site decreased promoter activity in XBP1s-transfected 1.1B4 cells from 138.534 ± 12.834 RLU to 107.342 ± 6.322 RLU ($P = 0.0032$) (Fig. 3G). Deleting these nucleotides further decreased promoter activity to 65.910 ± 4.7 RLU

CHOP expression was detected by mouse anti-CHOP monoclonal antibody. ATF4 was determined using rabbit anti-ATF4 polyclonal antibody. The ratio of cleaved (active) caspase 3/total caspase 3 was evaluated using cleaved caspase 3 (Asp175) antibody and caspase 3 (D3R6Y) rabbit monoclonal antibody, respectively. Internal control GADPH was analyzed using monoclonal antibody 14C10 (Cell signaling). Quantification of protein expression was performed by ImageJ software. The values represent mean ± standard error of the mean of three independent experiments ($n = 3$). $^{**}P < 0.01$, $^{****}P < 0.0001$ by student's *t*-test. The evaluations of hIAPP expressions were performed by ELISA **(C)** and by immunostaining **(D)**. **(E)** The DNA fragment was detected by TUNEL staining. **(D)** The representative pictures with an original magnification of X400 (insert (white lines): X1000). **(E)** The representative pictures with an original magnification of X200. Scar bar = 100 μm. The results were expressed as mean ± standard error of the mean of three independent experiments ($n = 3$). TUNEL-positive (apoptotic) β-cells in each condition were quantified. $^{*}P < 0.05$ by student's *t*-test. IAPP, islet amyloid polypeptide; IRE1, inositol requiring enzyme 1; CHOP, C/EBP homologous protein; ATF4, activating transcription factor 4.

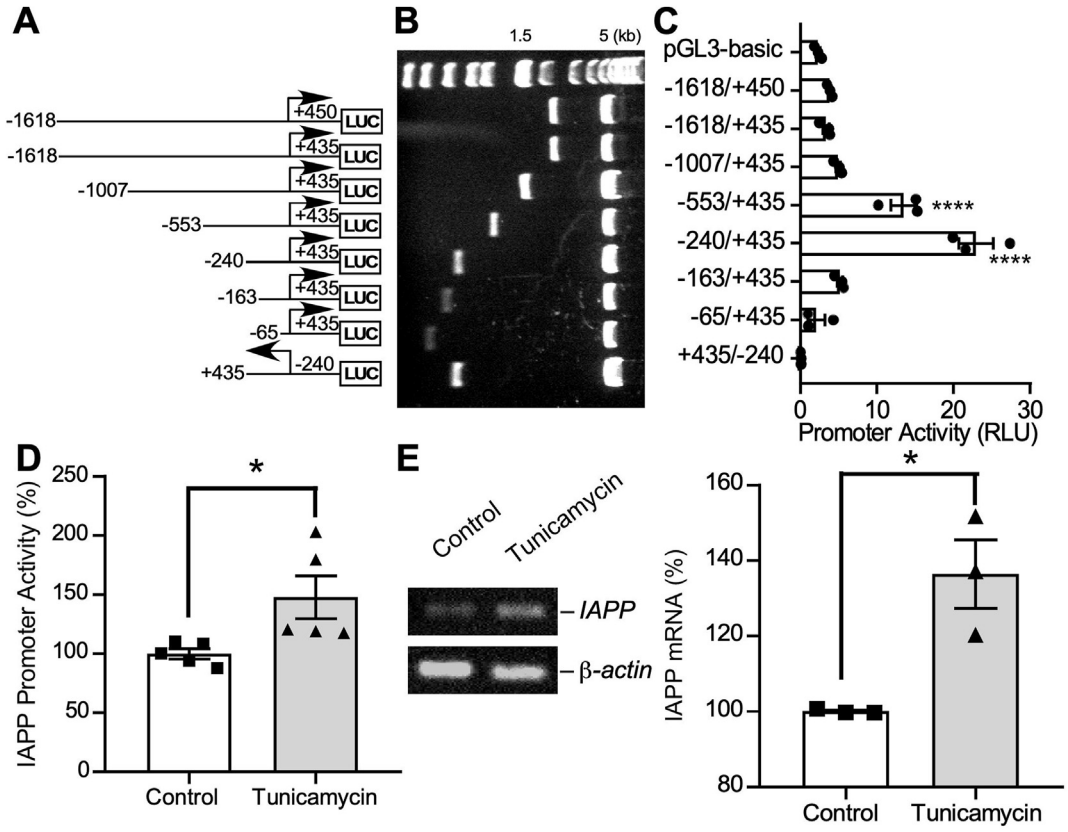

Figure 2 Tunicamycin enhances *hIAPP* transcription. **(A)** Schematic diagrams of cloned *hIAPP* promoter constructs, which consist of 5′ flanking regions with serial deletions inserted into the pGL3-basic vector. The arrows represent the transcription start site and direction of transcription, and the numbers represent the 5′ start and 3' end points of each construct relative to the transcription start site. **(B)** *hIAPP* promoter constructs were verified by restriction enzyme digest. Digested products were resolved on a 1% agarose gel and were further confirmed by sequencing. **(C)** Promoter deletion plasmids were co-transfected with pRL-CMV into 1.1B4 cells. Firefly luciferase activity was measured after 24 h and was expressed in relative light units (RLU). Renilla luciferase activity was used to normalize for transfection efficiency. EV, pGL3-basic empty vector control. The values represent mean ± standard error of the mean. $n = 4$ independent experiments; *$P < 0.05$ by one-way ANOVA with post-hoc Tukey's multiple comparisons test. **(D)** 1.1B4 cells were co-transfected with pIAPP-luc −553/+435 promoter fragment and pRL-CMV and treated with either 10 μg/mL tunicamycin or DMSO (controls) for 24 h. The values represent mean ± standard error of the mean of three independent experiments ($n = 3$). *$P < 0.05$ by student's *t*-test. **(E)** 1.1B4 cells were treated with either 10 μg/mL tunicamycin or DMSO for 24 h and RT-PCR was performed to determine *hIAPP* transcript levels normalized to β-actin. Band intensities were quantified by ImageJ software. $n = 3$; *$P < 0.05$ by student's *t*-test. IAPP, islet amyloid polypeptide.

($P < 0.0001$). In XBP1u-transfected 1.1B4 cells, neither the mutant (8.125 ± 0.423 RLU, $P > 0.9999$) nor deletion promoter constructs (7.736 ± 0.420 RLU, $P > 0.9999$) significantly changed promoter activity compared with the −240/+435 construct (7.874 ± 0.462 RLU) (Fig. 3G). More importantly, we also found that the deletion of the binding sites diminished the effect of ER stress on *hIAPP* promoter activity. The −240/+435 promoter construct with or without mutation displayed a significant increase in promoter activity in response to 24-h tunicamycin treatment compared with DMSO ($P = 0.0428$ and $P = 0.0221$, respectively) (Fig. 3H). However, tunicamycin treatment had no significant effect on the activity of the deletion construct ($P = 0.2985$) (Fig. 3H), suggesting that the deletion of the XBP1 binding site abolishes the effect of ER stress on *IAPP* transcription.

Inhibition of XBP1 improved ER stress-induced β-cell dysfunction

1.1B4 cells were treated with tunicamycin to induce ER stress, which increased hIAPP expression to 122% ± 2.52% ($P = 0.0010$) (Fig. 4A). We also examined β-cell function by assessment of insulin response to the elevated glucose level. After treatment with tunicamycin, human β-cells secreted significantly less insulin in response to the elevated glucose compared with the control cells (57.97% ± 1.95%, $P = 0.0017$) (Fig. 4B). These findings suggest that ER stress-induced hIAPP pathologies impair human β-cell survival and function.

MKC3946 binds to the endoribonuclease domain of IRE1α and therefore is widely used to block XBP1 mRNA splicing.[10] MKC3946 was added to the culture media 1 h before

tunicamycin treatment. MKC3946 treatment significantly inhibited ER stress-induced hIAPP expressions in human β-cells (110 ± 2.82 *vs.* 122 ± 2.52, $P = 0.0264$) (Fig. 4A). Furthermore, MKC3946 treatment significantly improved cell function to secrete more insulin in response to the elevated glucose level compared with the cells treated only

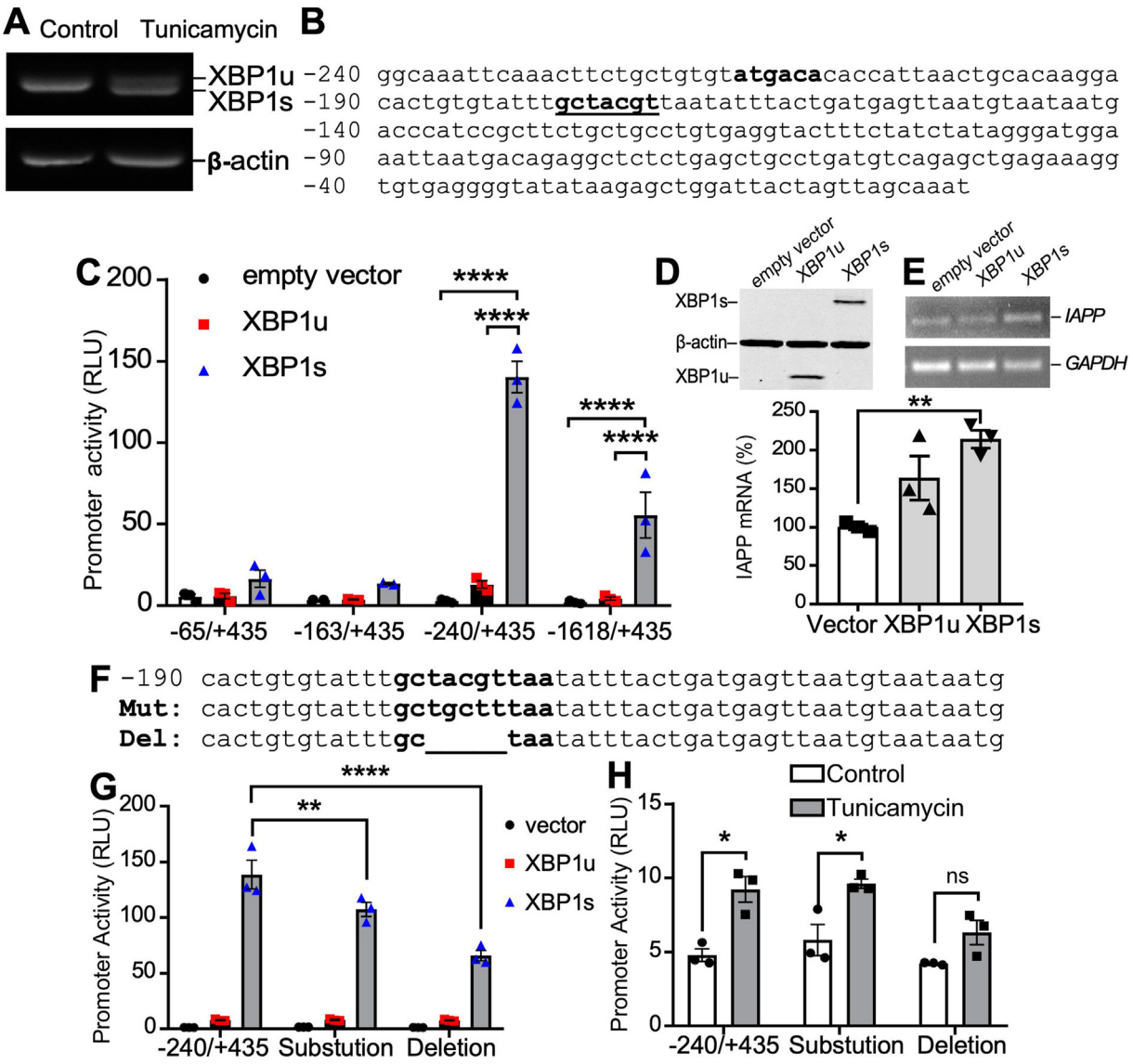

Figure 3 XBP1 up-regulates *IAPP* promoter activity. **(A)** 1.1B4 cells were treated with either 10 μg/mL tunicamycin or DMSO for 24 h and RT-PCR was performed to detect *XBP1* splicing. **(B)** The −240 to −1 region of the *hIAPP* promoter contains putative XBP1s binding sites. **(C)** *hIAPP* promoter constructs were co-transfected with pRL-CMV and either pcDNA4-mycHisA, XBP1u-myc, or XBP1s-myc into 1.1B4 cells and assayed for luciferase activity 24 h later. Firefly luciferase activity was expressed in relative light units (RLU) and values were normalized to Renilla luciferase activity to control for transfection efficiency. The values represent mean ± standard error of the mean. $n = 3$ independent experiments; $^{****}P < 0.0001$ by one-way ANOVA with Tukey's multiple comparisons test. 1.1B4 cells were transfected with either pcDNA4-mycHisA, XBP1u-myc, or XPB1s-myc plasmids **(D)** and RT-PCR was performed 24 h later to detect *hIAPP* mRNA expression normalized to *GAPDH* **(E)**. Band intensities were quantified by ImageJ software. The values represent mean ± sd ($n = 3$). $^{**}P < 0.01$ by one-way ANOVA with post-hoc Tukey's multiple comparisons test. **(F)** DNA sequences of the promoter fragment (top), mutation construct (mut), and deletion construct (del). **(G)** hIAPP promoter fragments −240/+435, mutant −240/+435, and deletion −240/+435 were co-transfected with pRL-CMV and either pcDNA4-mycHisA, XBP1u-myc, or XPB1s-myc plasmids into 1.1B4 cells. 24 h after transfection, cells were harvested for luciferase assay. **(H)** Plasmids were co-transfected with pRL-CMV into 1.1B4 cells for 12 h before the addition of either DMSO or 10 μg/mL tunicamycin for another 24 h before cells were harvested for luciferase assay. Firefly luciferase activity was expressed in relative light units (RLU) and values were normalized to Renilla luciferase activity to control for transfection efficiency. The values represent mean ± standard error of the mean ($n = 3$). $^{*}P < 0.05$ by two-way ANOVA with Sidak's multiple comparisons test. XBP1s, spliced X-box binding protein 1; hIAPP, human islet amyloid polypeptide.

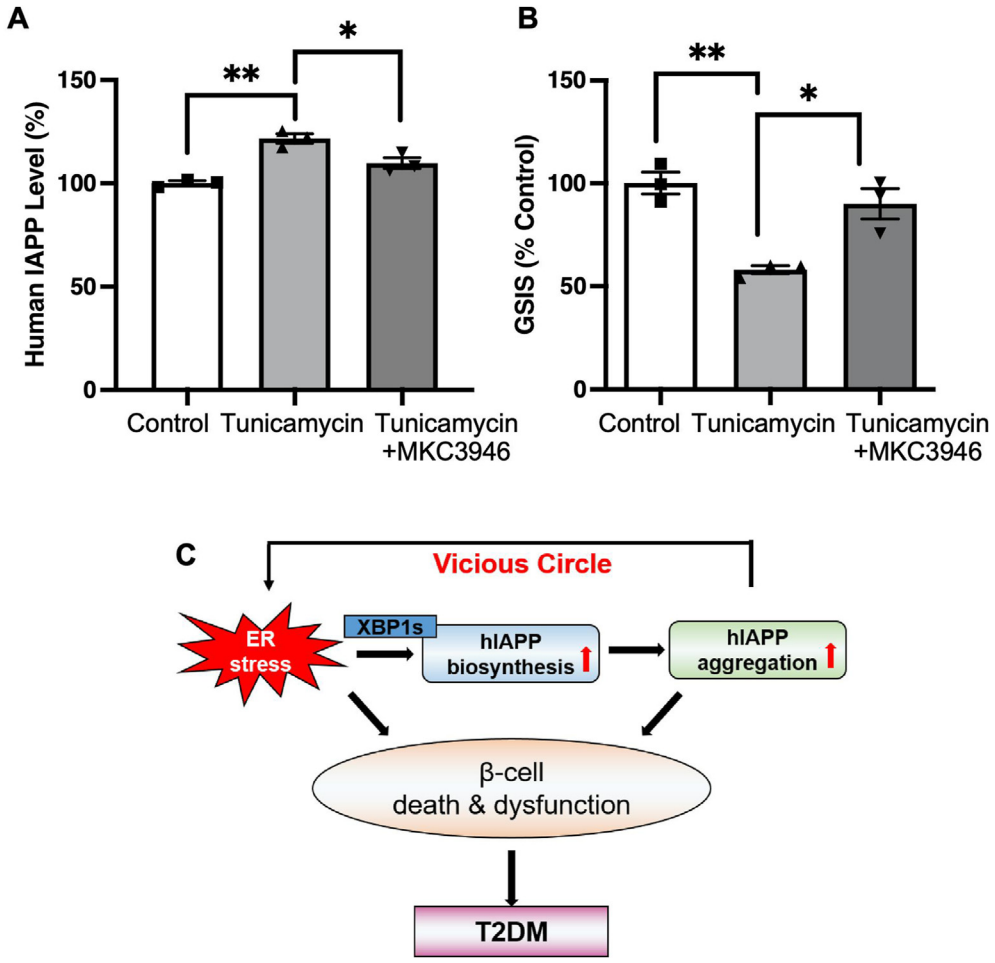

Figure 4 Blockade of XBP1 splicing by MKC3946 inhibits endoplasmic reticulum (ER) stress-induced hIAPP expression and improves β-cell dysfunction. **(A)** 1.1B4 cells were cultured with 10 μg/mL tunicamycin with or without MKC3946 treatment for 24 h. Culture media was collected to measure hIAPP levels by ELISA. **(B)** β-cell function was assessed by measuring glucose-stimulated (16.7 mmol/L) insulin secretion (GSIS). The results were expressed as mean ± standard error of the mean ($n = 3$). *$P < 0.05$, **$P < 0.01$ by one-way ANOVA with post-hoc Tukey's multiple comparisons test. **(C)** Schematic diagram of ER stress-induced hIAPP up-regulation and aggregation. ER stress enhances hIAPP promoter activity and biosynthesis by the activation of XBP1 splicing. The increased hIAPP level stimulates its aggregation, which may further amplify the ER stress to form a vicious circle, leading to β-cell death and dysfunction, and T2DM development. ER, endoplasmic reticulum; XBP1s, spliced X-box binding protein 1; hIAPP, human islet amyloid polypeptide; T2DM , type 2 diabetes mellitus.

with tunicamycin (89.92 ± 7.4 *vs*. 57.97 ± 1.95, $P = 0.014$) (Fig. 4B). These data indicate that inhibition of XBP1 improved ER stress-induced β-cell dysfunction (Fig. 4C).

Discussion

In patients suffering from T2DM, the reduction of β-cell area only occurs in islets with IAPP accumulation,[11] suggesting a significant pathological role for IAPP aggregation in the development of T2DM. IAPP is mainly produced in human pancreatic islet β-cells, and its promoter activity is regulated by several factors implicated in T2DM, such as hyperglycemia[12] and fatty acids.[13] In this study, we found that tunicamycin and thapsigargin, ER stress inducers, significantly increased *hIAPP* promoter activity and biosynthesis. An XBP1s binding site was identified in the *hIAPP* promoter at −177/−171 bp upstream of the transcription start site, and overexpression of XBP1s but not XBP1u significantly increased *hIAPP* transcription. Destruction of this putative binding site diminished the effects of tunicamycin treatment on *hIAPP* promoter activity, suggesting a key role for XBP1s in mediating *hIAPP* transcription induced by ER stress.

Activation of the UPR is a major adaptive response to ER stress through decreasing unfolded protein load. Out of the three branches of the UPR, activation of IRE1 is the most conserved.[14] Activation of IRE1α leads to its autophosphorylation and homodimerization, which allows it to act as an endoribonuclease to cleave its only known substrate, a mRNA encoding XBP1.[15] This unconventional splicing event leads to the removal of a 26 nucleotide intron and produces a spliced variant of XBP1 (XBP1s), which is a transcription factor that can initiate the transcription of UPR target

genes.[4,16] As a transcription factor, XBP1s recognizes a few different consensus sequences: a CCACG-box (GCCACG), UPRE sequences (CGACGTGG and GTGACGTG), an ACGT core (G(C/T) (C/G)ACGT), an ETS domain (CGGAAG), and a CAAT-box (CCAATC).[17] There are multiple predicted binding sites for XBP1s on the *hIAPP* promoter, but given that our −163 bp construct did not have a significant response to XBP1s overexpression, the putative functional sites are most likely between −240 and −163 bp. Within this region, there are two potential binding sites, ATGACAC and GCTACGT. Both sites have mismatched base pairs, but the latter has the important ACGT-core intact. Mutating part of the GCTACGT site significantly decreases the dramatic increase in *hIAPP* promoter activity in response to XBP1s overexpression. Deleting part of this site also diminishes the modest increase in promoter activity induced by ER stress. These results strongly indicate that XBP1s can directly regulate *hIAPP* promoter activity through the GCTACGT binding site. Both ATF4 and CHOP are also involved in the UPR, which is activated in response to ER stress. Thus, our results showed elevated levels of ATF4 and CHOP in cells treated with tunicamycin and thapsigargin. However, their roles in the IAPP production have not been extensively studied. ATF4 can modulate the expression of genes involved in lipid metabolism and oxidative stress, which makes it possible that ATF4 may indirectly affect the expression of genes involved in IAPP synthesis or secretion. CHOP is involved in the regulation of cell viability in response to prolonged or severe ER stress. Its involvement in modulating ER stress-induced apoptosis or protein degradation pathways may also indirectly influence IAPP levels. We are interested in doing some related studies in the future.

IAPP is known to regulate glucose homeostasis by influencing insulin secretion from β cells[18] and glucagon secretion from α cells.[19] However, overexpression of hIAPP leads to its aggregation and islet amyloid deposition,[7,20] which induces islet β-cell death and dysfunction.[21,22] Accordingly, we treated human β-cells with MKC3946, an IRE1α endoribonuclease domain inhibitor to block XPB1 mRNA splicing. Reduction of spliced XBP1 by MKC3946 treatment significantly inhibited ER stress-induced hIAPP expression and improved β-cell dysfunction induced by ER stress.

ER stress has been considered a major mechanism of hIAPP toxicity during T2DM.[23] In islets from human or hIAPP transgenic rodents, hIAPP oligomers induce β-cell apoptosis mediated by ER stress.[23,24] Deletion of CHOP, a major ER stress marker in hIAPP transgenic mice successfully reduces β-cell loss and defers diabetes development.[25] In this study, we discovered that ER stress enhanced *hIAPP* promoter activity, at least in part through XBP1 splicing. This change in *hIAPP* gene regulation also contributes to its biosynthesis and cytotoxic activity showing the reduced human β-cell survival and function. Our study revealed that ER stress may be triggered in β-cells during T2DM in a vicious circle in which ER stress will induce hIAPP pathology while the toxic consequences may further amplify the ER stress (Fig. 4C). Our novel findings will provide deep insights into the role of ER stress in T2DM pathogenesis. Since the IRE1α-XBP1 pathway plays an important role in ER stress-induced hIAPP up-regulation and aggregation, targeting and modulating this pathway may be a promising approach for T2DM therapy.

Author contributions

YZ and WS conceived and designed the experiments; YZ, SL, JY, CH, and AA performed the experiments; WC, YZ, SL, ZW, and WS analyzed and contributed reagents/materials/analysis tools; SL, YZ, and WS wrote the manuscript. YZ, ZW, and WS revised the manuscript. All authors reviewed the manuscript.

Data availability

All data generated or analyzed during this study are included in this published article.

Conflict of interests

The authors have declared that no conflict of interests exists.

Funding

This work was supported by the National Natural Science Foundation of China (No. 82201576), Beijing Hospitals Authority Youth Programme (China) (No. QML20210804), Beijing Medical Research 2021-8, Key Laboratory of Alzheimer's Disease of Zhejiang Province of China (No. ZJAD-2021004 to YZ), and the National Natural Science Foundation of China (No. 82230043 to WS). WS was the Canada Research Chair in Alzheimer's Disease. YZ and WS are the guarantors of this work and, as such, have full access to all the data in the study and take responsibility for the integrity of the data and the accuracy of the data analysis.

References

1. Ozcan U, Cao Q, Yilmaz E, et al. Endoplasmic reticulum stress links obesity, insulin action, and type 2 diabetes. *Science*. 2004;306(5695):457—461.
2. Back SH, Kaufman RJ. Endoplasmic reticulum stress and type 2 diabetes. *Annu Rev Biochem*. 2012;81:767—793.
3. Yoshida H, Haze K, Yanagi H, Yura T, Mori K. Identification of the cis-acting endoplasmic reticulum stress response element responsible for transcriptional induction of mammalian glucose-regulated proteins. *J Biol Chem*. 1998;273(50):33741—33749.
4. Yoshida H, Matsui T, Yamamoto A, Okada T, Mori K. XBP1 mRNA is induced by ATF6 and spliced by IRE1 in response to ER stress to produce a highly active transcription factor. *Cell*. 2001;107(7):881—891.
5. Allagnat F, Christulia F, Ortis F, et al. Sustained production of spliced X-box binding protein 1 (XBP1) induces pancreatic beta cell dysfunction and apoptosis. *Diabetologia*. 2010;53(6):1120—1130.
6. Opie EL. On the relation of chronic interstitial pancreatitis to the islands of Langerhans and to diabetes melutus. *J Exp Med*. 1901;5(4):397—428.

7. Janson J, Soeller WC, Roche PC, et al. Spontaneous diabetes mellitus in transgenic mice expressing human islet amyloid polypeptide. *Proc Natl Acad Sci U S A*. 1996;93(14):7283—7288.
8. Zhang Y, Song W. Islet amyloid polypeptide: another key molecule in Alzheimer's pathogenesis? *Prog Neurobiol*. 2017; 153:100—120.
9. Marzban L, Tomas A, Becker TC, et al. Erratum. small interfering RNA-mediated suppression of proislet amyloid polypeptide expression inhibits islet amyloid formation and enhances survival of human islets in culture. *Diabetes*. 2008; 57:3045—3055. Diabetes. 2016;65(3):818.
10. Mimura N, Fulciniti M, Gorgun G, et al. Blockade of XBP1 splicing by inhibition of IRE1α is a promising therapeutic option in multiple myeloma. *Blood*. 2012;119(24):5772—5781.
11. Jurgens CA, Toukatly MN, Fligner CL, et al. β-cell loss and β-cell apoptosis in human type 2 diabetes are related to islet amyloid deposition. *Am J Pathol*. 2011;178(6):2632—2640.
12. Gasa R, Gomis R, Casamitjana R, Rivera F, Novials A. Glucose regulation of islet amyloid polypeptide gene expression in rat pancreatic islets. *Am J Physiol*. 1997;272(4 Pt 1): E543—E549.
13. Qi D, Cai K, Wang O, et al. Fatty acids induce amylin expression and secretion by pancreatic beta-cells. *Am J Physiol Endocrinol Metab*. 2010;298(1):E99—E107.
14. Welihinda AA, Kaufman RJ. The unfolded protein response pathway in *Saccharomyces cerevisiae*. Oligomerization and trans-phosphorylation of Ire1p (Ern1p) are required for kinase activation. *J Biol Chem*. 1996;271(30):18181—18187.
15. Cox JS, Walter P. A novel mechanism for regulating activity of a transcription factor that controls the unfolded protein response. *Cell*. 1996;87(3):391—404.
16. Calfon M, Zeng H, Urano F, et al. IRE1 couples endoplasmic reticulum load to secretory capacity by processing the XBP-1 mRNA. *Nature*. 2002;415(6867):92—96.
17. Acosta-Alvear D, Zhou Y, Blais A, et al. XBP1 controls diverse cell type- and condition-specific transcriptional regulatory networks. *Mol Cell*. 2007;27(1):53—66.
18. Ohsawa H, Kanatsuka A, Yamaguchi T, Makino H, Yoshida S. Islet amyloid polypeptide inhibits glucose-stimulated insulin secretion from isolated rat pancreatic islets. *Biochem Biophys Res Commun*. 1989;160(2):961—967.
19. Åkesson B, Panagiotidis G, Westermark P, Lundquist I. Islet amyloid polypeptide inhibits glucagon release and exerts a dual action on insulin release from isolated islets. *Regul Pept*. 2003;111(1—3):55—60.
20. Bailey J, Potter KJ, Verchere CB, Edelstein-Keshet L, Coombs D. Reverse engineering an amyloid aggregation pathway with dimensional analysis and scaling. *Phys Biol*. 2011;8(6):066009.
21. Zhang Y, Jalili RB, Warnock GL, Ao Z, Marzban L, Ghahary A. Three-dimensional scaffolds reduce islet amyloid formation and enhance survival and function of cultured human islets. *Am J Pathol*. 2012;181(4):1296—1305.
22. Zhang Y, Warnock GL, Ao Z, et al. Amyloid formation reduces protein kinase B phosphorylation in primary islet β-cells which is improved by blocking IL-1β signaling. *PLoS One*. 2018;13(2): e0193184.
23. Matveyenko AV, Gurlo T, Daval M, Butler AE, Butler PC. Successful versus failed adaptation to high-fat diet-induced insulin resistance: the role of IAPP-induced beta-cell endoplasmic reticulum stress. *Diabetes*. 2009;58(4):906—916.
24. Huang CJ, Lin CY, Haataja L, et al. High expression rates of human islet amyloid polypeptide induce endoplasmic reticulum stress mediated beta-cell apoptosis, a characteristic of humans with type 2 but not type 1 diabetes. *Diabetes*. 2007; 56(8):2016—2027.
25. Gurlo T, Rivera JF, Butler AE, et al. CHOP contributes to, but is not the only mediator of, IAPP induced β-cell apoptosis. *Mol Endocrinol*. 2016;30(4):446—454.